Journal of Intelligent Systems and Control
https://www.acadlore.com/journals/JISC

Neuro-Fuzzy Logic Controller for Switching Capacitor Banks in Power Factor Correction within the Manufacturing Industry

Olamide Omolara Olusanya[1], Gbenga Mufutau Adebajo[2], Ibrahim Giwa[3], Kennedy Okokpujie[4*], Samuel Adebayo Daramola[4], Adenugba Vincent Akingunsoye[5]

[1] Department of Computer Engineering, Bells University of Technology, 112212 Ota, Nigeria
[2] Department of Electrical/Electronics and Telecommunication Engineering, Bells University of Technology, 112212 Ota, Nigeria
[3] College of Engineering, Bells University of Technology, 112212 Ota, Nigeria
[4] Department of Electrical and Information Engineering, College of Engineering, Covenant University, 112212 Ota, Nigeria
[5] Directorate OVA Foundation, 21651 Millington, USA

[*] Correspondence: Kennedy Okokpujie (kennedy.okokpujie@covenantuniversity.edu.ng)

Received: 03-23-2024 **Revised:** 06-08-2024 **Accepted:** 06-21-2024

Citation: O. O. Olusanya, G. M. Adebajo, I. Giwa, K. Okokpujie, S. A. Daramola, and A. V. Akingunsoye, "Neuro-fuzzy logic controller for switching capacitor banks in power factor correction within the manufacturing industry," *J. Intell Syst. Control*, vol. 3, no. 2, pp. 93–106, 2024. https://doi.org/10.56578/jisc030203.

Abstract: Regulatory bodies in electrical engineering mandate the installation of power factor (PF) improvement systems to elevate PF values to between 0.9 and 0.96. Compliance is enforced by regional or local utility companies through penal rates and incentives for PF values nearing unity. Traditional power factor correction (PFC) systems often utilize microprocessor-based controllers for switching capacitor banks, which can result in under- or over-compensation of reactive power. This study developed an adaptive neuro-fuzzy inference system (ANFIS) utilizing a Sugeno-Takagi inference model based on the sub-clustering method to address the limitations of sensitivity and response time observed in existing microcontroller-based PFC systems. The proposed neuro-fuzzy (NF) controller comprises a five-layered model with two inputs, i.e., kilowatt (KW) and kilovolt-ampere reactive (KVAR), and one output (PF). A 25-rule set performance of the developed program was achieved, with significant improvements observed after 50 epochs, culminating in an error rate of 0.050691 recorded post the second epoch. The results demonstrated that the developed controller exhibits higher sensitivity and faster response time compared to existing PF controllers. Consequently, the implementation of the proposed controller is recommended for optimizing the switching of capacitor banks, thereby enhancing PF in manufacturing industries characterized by variable load conditions.

Keywords: Power factor correction; Power factor; Capacitor; Fuzzy capacitor bank; Adaptive neuro-fuzzy inference system; Artificial neural network; Energy efficiency; Industrial applications

1 Introduction

In an electrical system, the total power called apparent power is the combination of real power (useful power) and reactive power (the power that oscillates back and forth between the source and the load without performing any work) [1, 2]. The consumption of apparent power results from the presence of reactive loads, which introduce a phase difference between the voltage and current waveforms. This phase difference is a critical determinant of the PF, a measure that signifies the efficiency of power utilization in the system. Optimizing PF, especially in industrial settings, is crucial for enhancing energy efficiency and minimizing electrical losses [3, 4].

About 60% of industrial loads (mostly inductive loads) exhibit a lagging PF, leading to greater apparent power than the real power since the current lags behind the voltage [5, 6]. A low PF, often caused by inductive loads, results in increased reactive power consumption and heightened demand on the power distribution infrastructure [7]. Most electric motors, especially in the manufacturing subsector, operate at lower design loading and, on average, operate between 60% and 80% of their full load [8, 9].

The economic ramifications of poor PF are significant. In line with the Institute of Electrical and Electronics Engineers (IEEE) standard 519 and other relevant International Electro-technical Commission (IEC) specifications, many utility companies impose penalties on industrial consumers operating below the 0.95 or 0.9 PF thresholds [10]. These penalties typically manifest as stringent electricity tariffs.

To address this, this current study employs capacitor banks as a reactive power compensation method integral to PFC. Notably, a neuro-fuzzy logic (FL) controller was proposed for its switching technique, aiming to improve the sensitivity and effectiveness of the PFC techniques compared to other methods.

2 Review of PFC Methods

Generally, PFC methods/techniques are classified into active and passive types. The former uses active switches and direct current-direct current (DC-DC) converters, which have different topologies. Out of the active methods, the conventional boost, buck-boost, synchronous compensators, and bridgeless converters have been known for their significant PFC improvements. In research conducted by Saini et al. [10], the bridgeless boost converter was shown to achieve the lowest total harmonic distortion (THD) of 5.44% when compared to conventional boost and full-bridge rectifier converters, which showed a THD value of 18.84% and 28.32%, respectively. Kumar Injeti et al. [11] proposed a new control strategy using only one PFC boost converter connected in a shunt with a diode rectifier that produced less than 5% of THD. This control method used the current error amplifier as part of the feedback loop to sense and filter the inductor current, thereby reducing the error between the average input current and the reference value. However, this method is limited to applications with low and fixed non-linear load currents.

On the other hand, passive PFC employs components such as capacitor banks, reactors, and filters to enhance the PF in electrical systems. This method utilizes the inductor-capacitor (L-C) filter to reduce the harmonics and regulate reactive power, thereby improving the PF. The capacitor banks have been shown to give the best PF improvement based on recent research because they are simple, bulky, rugged, and easy to install, and they can be used with detuned inductors to reduce the spread of harmonic current [12]. Static shunt capacitors are generally preferred to static series capacitors as the latter generates a high over-voltage when fault currents flow through them.

2.1 PFC Capacitor Bank Placement

The optimal PFC results are attained when these shunt capacitors are strategically placed for KVAR compensation, as emphasized by Olabode et al. [13]. Capacitor placement involves using optimization algorithms to identify a location in the system for the capacitors and the size of the capacitor to be installed at the identified location. The benefits of properly placing capacitors in the distribution network are bus voltage regulation, power loss reduction, power system component capacity release, PF improvement, and power quality management improvement [14]. Many researchers have been able to prove this assertion.

A good example is the work of Kumar et al. [15], where the problem of optimal capacitor placement and sizing was resolved by using the firefly algorithm (FFA) and the backtracking search algorithm (BSA). The solution was shown with recorded loss minimization, maximization of the annual cost savings, improved voltage profile, and improved power quality. Shunt capacitors for PFC can be connected directly across the terminals of inductive loads, especially when the power rating of the load is relatively smaller and across groups of loads in different locations, as shown in Figure 1, depending on the type of installation required [16]. For example, Location A is applied to a new motor installation in which the thermal overload relay can be sized with reduced current drawn. Location B is used for the line side of the overload relay. In contrast, Location C is required for motors with high inertia, where disconnecting the motor with the capacitor can turn the electric motor into a self-excited generator. This location (C) is preferred when the motor is frequently jogged, plugged, or reversed.

2.2 APFC Capacitor Controllers

The automatic PFC (APFC) controller switches on or off, or blocks PF capacitors depending on the amount of KVAR compensation needed [8]. The use of such a controller solves some potential problems that include increased harmonic distortion, transient over-voltage, under-compensation, and overcompensation. The PF controller can control the individual PF capacitors in steps, depending on the variation in electrical loads. The sensors for sampling the current circuit voltage and current to calculate the prevailing PF are current transformers.

The most commonly used methods to switch capacitor banks for PFC are programmable logic controllers (PLC), proportional integral and derivative (PID) controllers, Arduino controllers, microprocessor-based controllers, artificial neural network (ANN)-based controllers, and FL controllers. Mane et al. [17] used the ATMEGA328 microcontroller to control the capacitor bank. The system utilizes a PF transducer as a sensing device, interfaced with a microcontroller unit (MCU), to correct the PF. The MCU, based on the PF value, controls the relay to either normally close or open, activating the capacitor bank. While this approach effectively improves the PF to 0.9, a notable drawback is its limited efficiency for large-scale implementation, making it more suitable as a prototype.

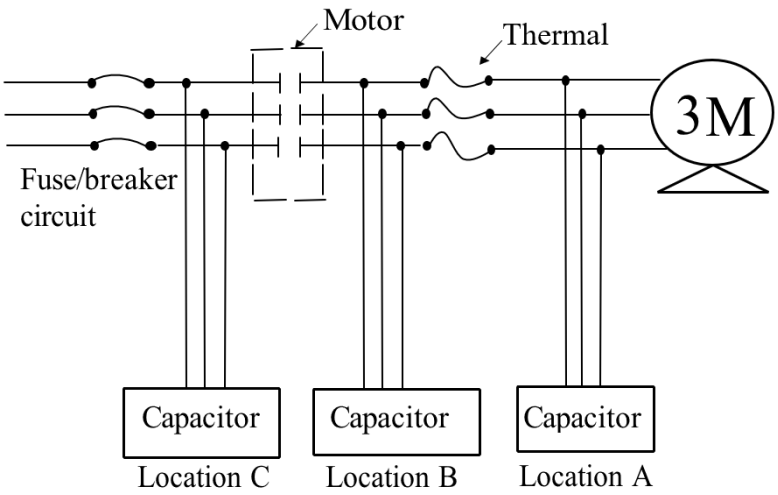

Figure 1. Various placements of capacitor banks

Kayisli et al. [18] employed the use of a Sliding Mode (SM)-FL system to mitigate the effects of chattering in microprocessors of a PFC control algorithm. The system successfully generated pulse width modulation (PWM) signals by converting real-time codes through the MATLAB-dSpace Real-Time Interface, loading these codes into the program memory of the DS1103 digital signal processor (DSP). The study achieved a PF of 0.993 and a THD value of 3.9% under a 4A input current condition while acknowledging the system's limitations and stating the need for a fast DSP for future implementation.

Widjonarko et al. [1] simulated a control algorithm using MATLAB Simulink in two steps. Firstly, the system was designed to detect lagging and leading PFs using a D flip-flop (known as the power saturation block), whose output was combined using an OR gate. The relay and capacitor unit further controlled it via the ANN model to respond to and actuate any change in the power saturation block. The ANN structure consists of the error as the first input, the delta error as the second input, and a change in response value as the output, resulting in a training accuracy of 0.99758. To validate the system's performance, it checked for adaptation to changes in capacitor value, demonstrating superior performance compared to conventional methods based on response time.

Durgadevi and Umamaheswari [19] proposed another method for PFC and designed an automatic PF controller circuit using FL. In this work, a 1.5 KW single-phase induction motor was used in an experiment involving two sets of capacitor banks. The sizes of capacitors used were selected from a multiplier table using the obtained k-factor along with the initial PF of 0.644 lagging. The researchers achieved a PF of 0.997 when the first capacitor bank was switched on and a leading PF of 0.364 when the sets of two capacitor banks were switched on. However, in a study that looks similar to the method proposed in this current study, Karaboga and Kaya [20] designed a system that utilized the DC-DC single-ended primary inductance converter (SEPIC), proportional integrator (PI) controller, and ANFIS model for current mode control in a single-phase PFC. Initially, the alternating current (AC) input was rectified, and then the DC-DC SEPIC converter was employed as the sensing component. The PI controller and ANFIS model subsequently regulated the output to generate the necessary PWM pulses, which achieved an efficiency of 94.6% and a THD value of 1.678%. This study aims to improve the accuracy of the aforementioned PFC controllers using ANFIS as a control system for capacitor banks.

The major contributions of this study are as follows:

i. The actual dataset was collected from an already-installed microcontroller PFC capacitor bank.

ii. A neuro-FL algorithm based on the sub-clustering method was developed to control the capacitor banks of PFC.

iii. The result of the proposed model was predicted using the actual dataset.

iv. The proposed model was compared with artificial intelligence (AI) models such as FL and ANN.

3 Methodology

This study proposed an already existing neuro-FL algorithm for controlling capacitor banks necessary for PFC. Several efforts have been made to correct the PF. In all these efforts, the combination of the FL controller and the ANN-based controller for PFC has not been reported. Rather, emphasis was placed on only one controller at a time. To mitigate the drawbacks of an ANN-based controller and a FL controller, this study combined the two natural tools to form a neuro-FL controller and used it for PFC through static shunt capacitors installed and controlled in a sequence of steps.

Figure 2 shows the block diagram and workflow of the proposed model. Firstly, actual data was collected from an existing microcontroller-based PFC, and then the data was checked and cleaned for missing data. The resulting dataset was passed to the neuro-FL model after splitting into training, testing, and validation datasets. The trained model serves as the controller to actuate the capacitor banks (connected in a delta 3-phase line) and the relays to provide a faster response switching system for capacitor banks.

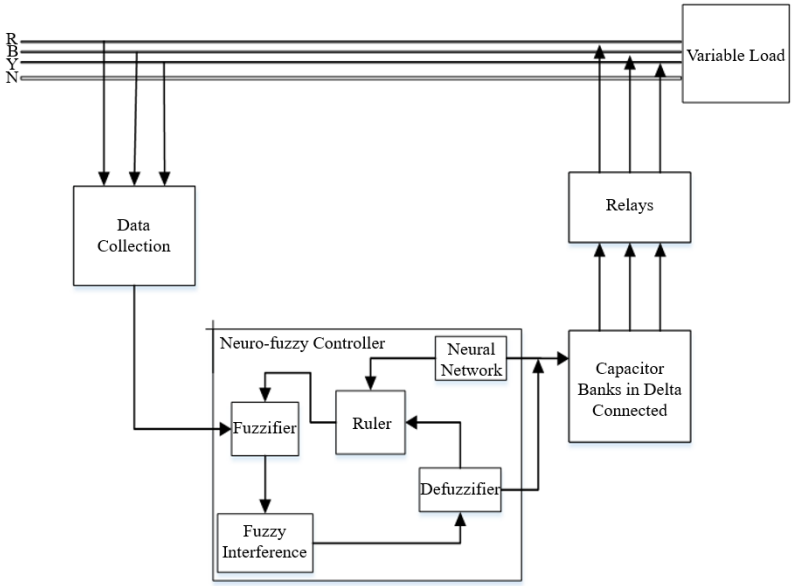

Figure 2. Block diagram of the proposed model

3.1 Data Collection

The dataset used in this study was obtained from the two milling machines in the manufacturing industry, utilizing existing microprocessor-based PFC sequence controllers, as illustrated in Figure 3. Initially, the controller measures line current and line voltage using current and voltage transformers. Subsequently, it rectifies and conditions the variables through zero-crossing detectors, supplying five volts to the micro-controller terminals. The phase angle, derived from the delay between line quantities, was captured using the internal timer register. The internal timer, calibrated from 0 to 5 ms to represent a 0-90-degree phase angle, generates the system PF at various electrical loading levels. This PF was then compared with the pre-set desired PF displayed on the controller's faceplate (Figure 4). The difference was now used to control the output of the PFC microcontroller after a predefined checking time before the capacitors were switched accordingly through the control relays and capacitors. The input features of the dataset consist of KW and KVAR, while PF represents the output variable for two milling machines in the industry. The collected primary data was divided into three sets: training, testing, and validation.

3.2 Neuro-FL Algorithm

The ANFIS, one of the common types of neuro-FL, was adopted in this study. This NF system uses a learning algorithm to determine its major parameters (such as fuzzy sets, fuzzy rules, etc.) by processing various data samples. As shown in Figure 2 and Figure 5, it has five layers, comprising two inputs and one output. Layer 1, known as the fuzzifier, uses membership functions to obtain fuzzy clusters from input [20]. In this layer, the premise parameter sets $\{a, b, c\}$, which determine the membership function, are given in Eq. (1) and Eq. (2) below, where μx and μy represent the membership degrees.

$$\mu_{A_i}(x) = \text{gbelln}\, f(x; a, b, c) = \frac{1}{1 + \left|\frac{x-c}{a}\right|^{2b}} \tag{1}$$

$$O_i^1 = \mu_{A_i}(x) \tag{2}$$

$$O_i^2 = w_i = \mu_{A_i}(x) * \mu_{B_i}(y) i = 1, 2 \tag{3}$$

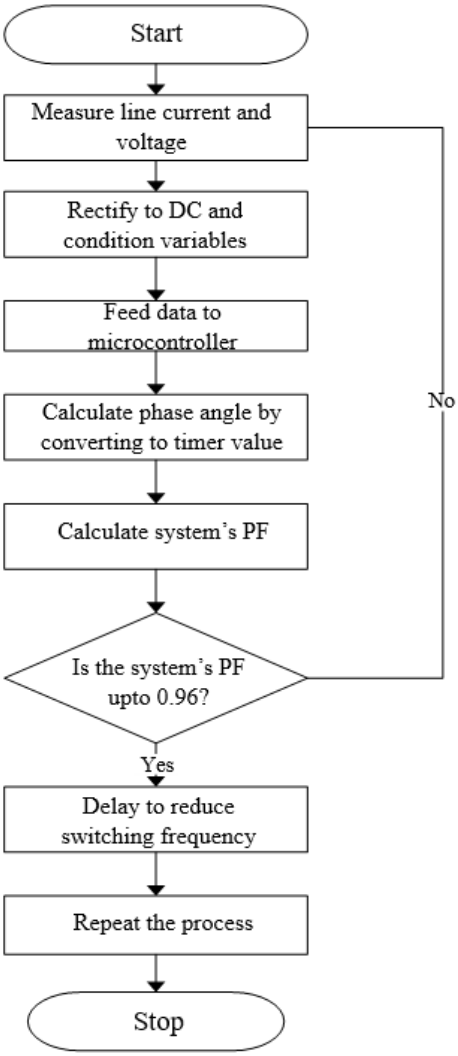

Figure 3. Flowchart of dataset collection

Figure 4. Faceplate of PFC sequence controllers

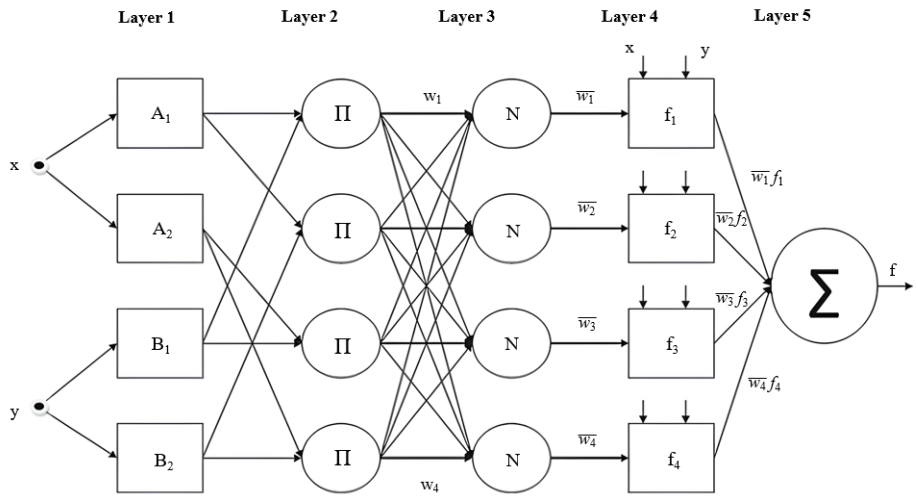

Figure 5. ANFIS model

$$o_i^3 = \overline{w_l} = \frac{w_i}{w_1 + w_2 + w_3 + w_4} \quad i \in \{1, 2, 3, 4\} \tag{4}$$

$$O_i^4 = \overline{w_l} f_i = \overline{w_l} \left(p_i x + q_i y + r_i\right) \tag{5}$$

$$O_i^5 = \sum_i \overline{w_l} f_i = \frac{\sum_i w_i f_i}{\sum_i w_i} \tag{6}$$

Furthermore, Layer 2, known as the ruler layer, obtains the firing strengths (w_i), computed as given in Eq. (3). Layer 3, called the normalization layer, calculates the normalized firing strengths of each rule, as given in Eq. (4). Layer 4, known as the de-fuzzifier, calculates the weighted values of each node in the rules using a first-order polynomial, as given in Eq. (5). Lastly, Layer 5, called the summation layer, obtains the actual output by summing the values of each rule in Layer 4, as given in Eq. (6).

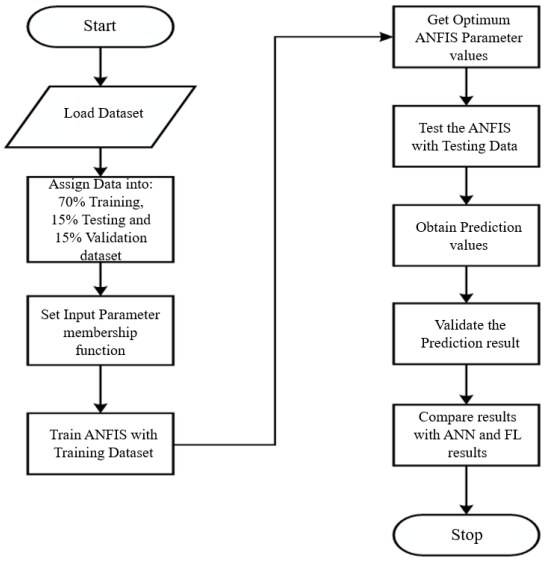

Figure 6. Proposed ANFIS algorithm

As shown in Figure 6, this algorithm utilizes the dataset (with input features of KW and KVAR) from an existing microcontroller capacitor bank, which first split the dataset into 70% training, 15% testing, and 15% validation datasets to enhance the accuracy of the ANFIS model. The model was initialized using the sub-clustering method,

based on the Gaussian function as given in Eq. (7), to estimate the density around each data point.

$$\emptyset\left(x, c_i\right)=\exp\left(-\frac{\left\|x, c_i\right\|^2}{2\sigma_i^2}\right) \tag{7}$$

where, $\emptyset\left(x, c_i\right)$ is the Gaussian function representing the density of data point x around the cluster center, c_i $\left\|x, c_i\right\|^2$ is the squared Euclidean distance between data point x around the cluster center c_i, and σ_i is a parameter that controls the spread of the Gaussian function.

3.3 Calculation of a PFC Capacitor Bank

Capacitor banks compensate the active power (P) from a PF $\tan\varphi_1$ to a PF $\tan\varphi_2$, as calculated in Eq. (8). In industrial plants, it can be assumed that the primaly inductive loads operate with an average PF of less than or equal to 0.7 . Therefore, an average of 50% of active power must be compensated for PF between 0.9 and 0.95 , as shown in Figure 7.

$$Q_c=P*(\tan\varphi_1-\tan\varphi_2) \tag{8}$$

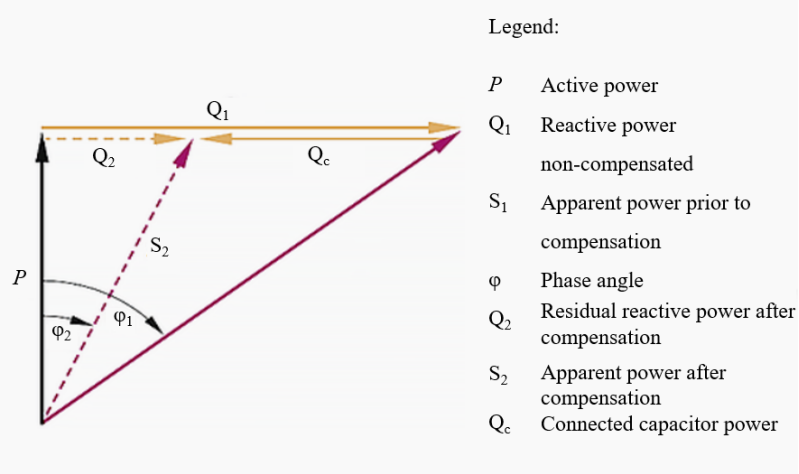

Figure 7. Relationship between P, S, and Q

The apparent power (S in KVA) is the vectorial sum of the active power (P in KW) and the reactive power (Q in KVAR) mathematically, as shown in Eqs. (9)-(12).

$$P=Q*PF(\cos\theta) \tag{9}$$

$$Q(KVAR)=\sqrt{3}*V*I*\sin\theta(3-\text{phase}) \tag{10}$$

$$Q_c=P*(\tan\varphi_1-\tan\varphi_2) \tag{11}$$

$$S(KVA)=\sqrt{(KW)^2+(KVAR)^2} \tag{12}$$

where, V is the supply voltage, I denotes the supply current, and θ is the phase angle between V and I. For industries, capacitor banks, which are mostly installed in central compensation form, utilize a controller system below.

As shown in Figure 8, the capacitors are switched in a sequence of steps, depending on the number of these steps.

For instance, a compensation unit of 110 KVAR might have four capacitors with a ratio of 1:2:4:4, amounting to 11 steps in total. In this study, shunt capacitor banks in central group form have been shown to give the best performance with the ANFIS controller because it is not only economical but also easy to install and flexible to operate in non-linear loads. As shown in Figure 8, the capacitor banks are connected in parallel using a 3-phase delta connection. However, the basic equation for calculating the size of capacitor banks is given as follows:

$$C=Q/(V*2*f) \tag{13}$$

where, C is the capacitance in Farad (F), Q denotes the reactive power in VAR, V is the voltage in volts (V), and f denotes the frequency in hertz (Hz).

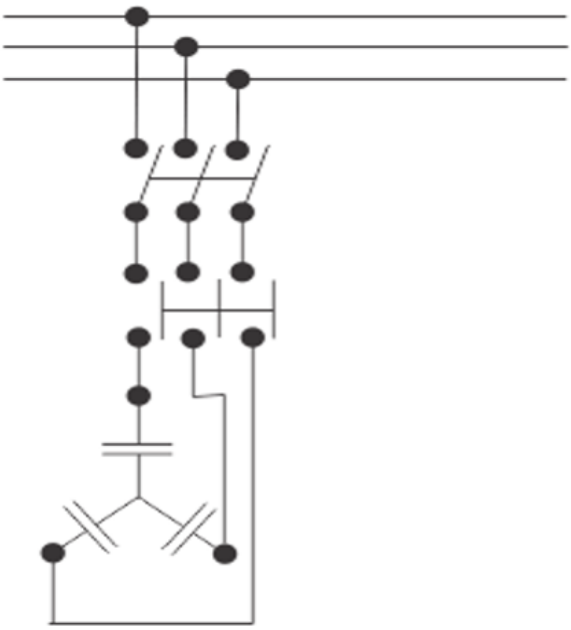

Figure 8. Delta-connected capacitor

4 Results and Discussion

This section shows the analysis and prediction results of the ANFIS, ANN, and FL models on MATLAB Software R2018a.

4.1 Results of the ANFIS Model

The ANFIS model was trained with the 'trail' transfer function using 35 nodes, 9 fuzzy rules, and 27 parameters, which include 9 linear parameters and 18 nonlinear parameters, as shown in Table 1. In addition, in Table 2, the training process involved two epochs, and the designated epoch number was reached during each training iteration, indicating that ANFIS training was completed at Epoch 2, which suggests efficient convergence. The subgraphs (a)-(f) of Figure 9 show the ANFIS data loading interface, design architecture, training error interface, design test interface, design rule viewer, and surface plot for ANFIS, respectively. The sub-clustering method helps to improve the response speed of the controller at just the 2nd iteration out of 50 initially programmed. The predicted results showed 95% accuracy, with a root mean square error (RMSE) value of 0.050691. This 95% accuracy has major advantages for industrial sectors regarding efficiency, cost savings, equipment protection, and regulatory compliance. The developed ANFIS model, used to swap capacitor banks for PFC, has a low RMSE value of 0.050691. This indicates good accuracy, precision, and reliability. All of these are used for optimizing energy management in industrial businesses.

Table 1. ANFIS training parameters

ANFIS Information	Parameter
Number of nodes	35
Number of linear parameters	9
Number of nonlinear parameters	18
Total number of parameters	27
Number of training data pairs	23
Number of checking data pairs	0
Number of fuzzy rules	9

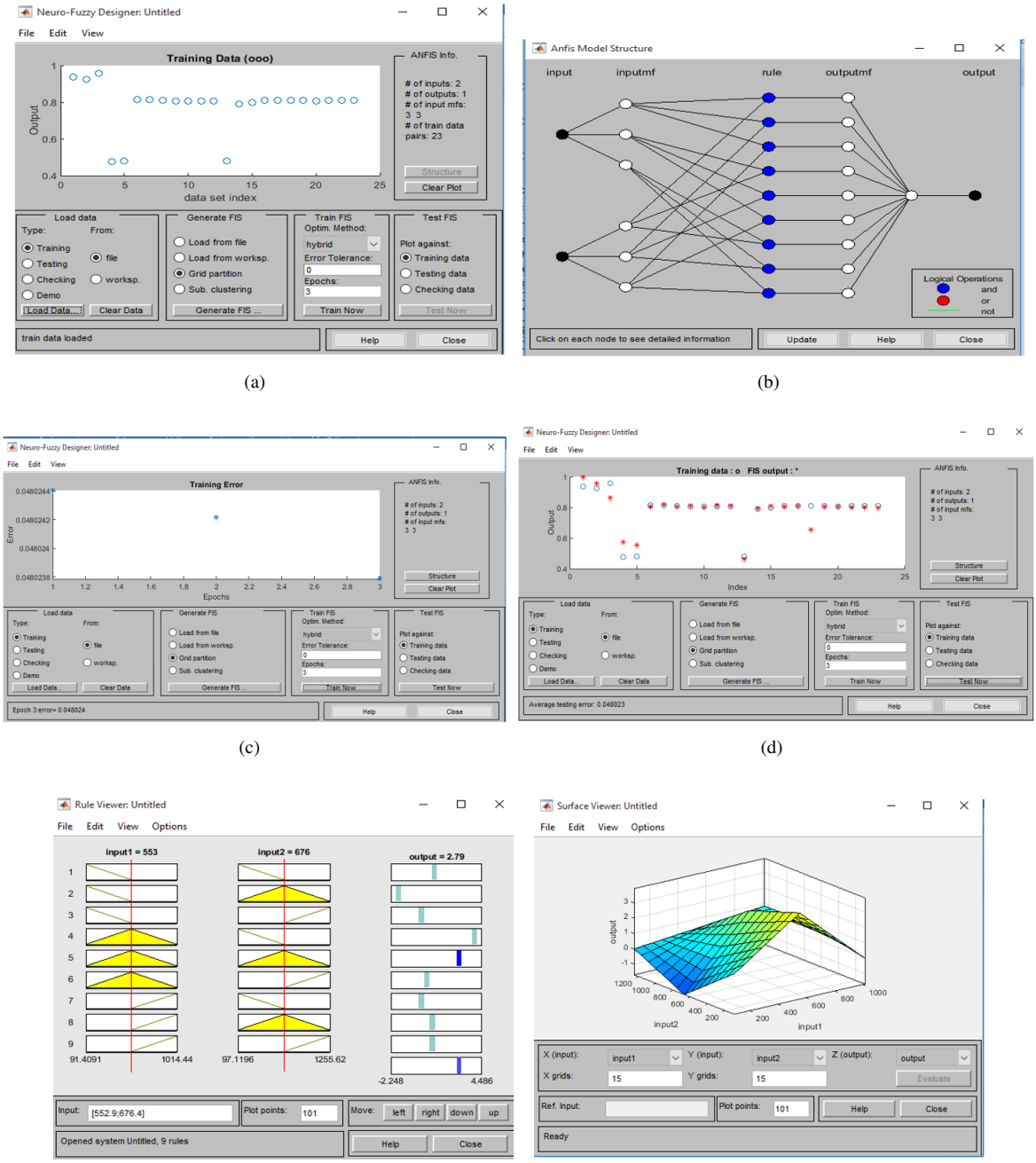

Figure 9. (a) Data loading interface; (b) Design architecture; (c) Training error interface; (d) Test data interface; (e) Design rule viewer; (f) Surface plot

Table 2. ANFIS training result

Training Result	Epoch 1	Epoch 2
Start training	-	-
RMSE of ANFIS training	0.0480242	0.0480238
Designated epoch being reached or not	Yes	Yes
RMSE of minimal training	0.048024	0.048023

4.2 Comparison with Other Models

The ANFIS model was compared with both the ANN and FL models, which had the same dataset ratio as ANFIS. The ANN prediction was performed in the ANN MATLAB Toolbox using the "Levenberg-Marquardt" algorithm,

as shown in Figure 10 and Figure 11.

An optimum neuron of 20 resulted in a high correlation coefficient (R-value) of 0.86554 for the training, 0.95752 for the validation, an overall R-value of 0.90372, and a low Mean Squared Error (MSE) value of 0.000037944, as shown in Figure 12 and Figure 13. In addition, the MSE (performance) plots in Figure 13 indicate the tolerance level and training failure even at the optimum number of 20 neurons. However, the training plots in Figure 14 indicate a learning rate (mu) of 0.01 for each result, a validity check achieved at 7, and an epoch number of 64. The increased number of epochs has been shown to enhance both the training and validation phases of the ANN algorithm, thereby improving overall performance.

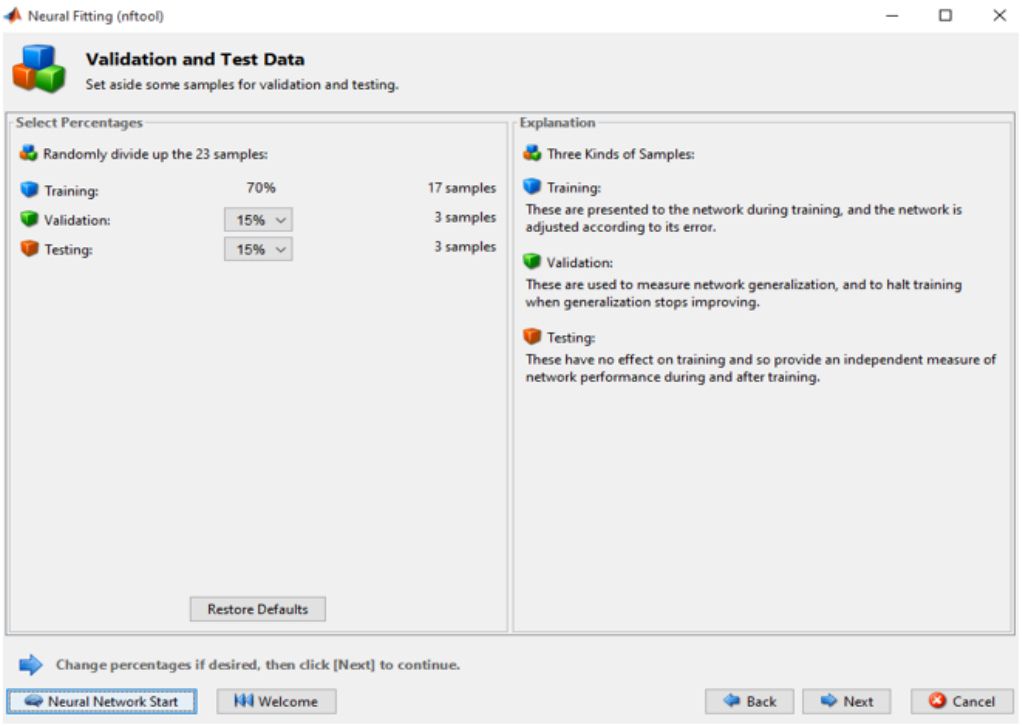

Figure 10. ANN data division interface

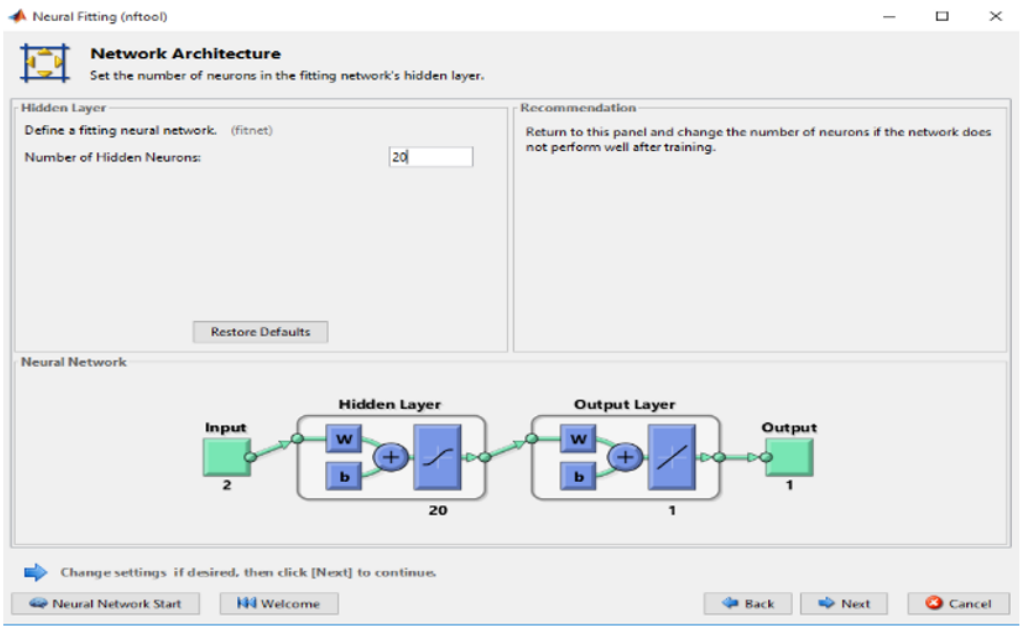

Figure 11. ANN architecture

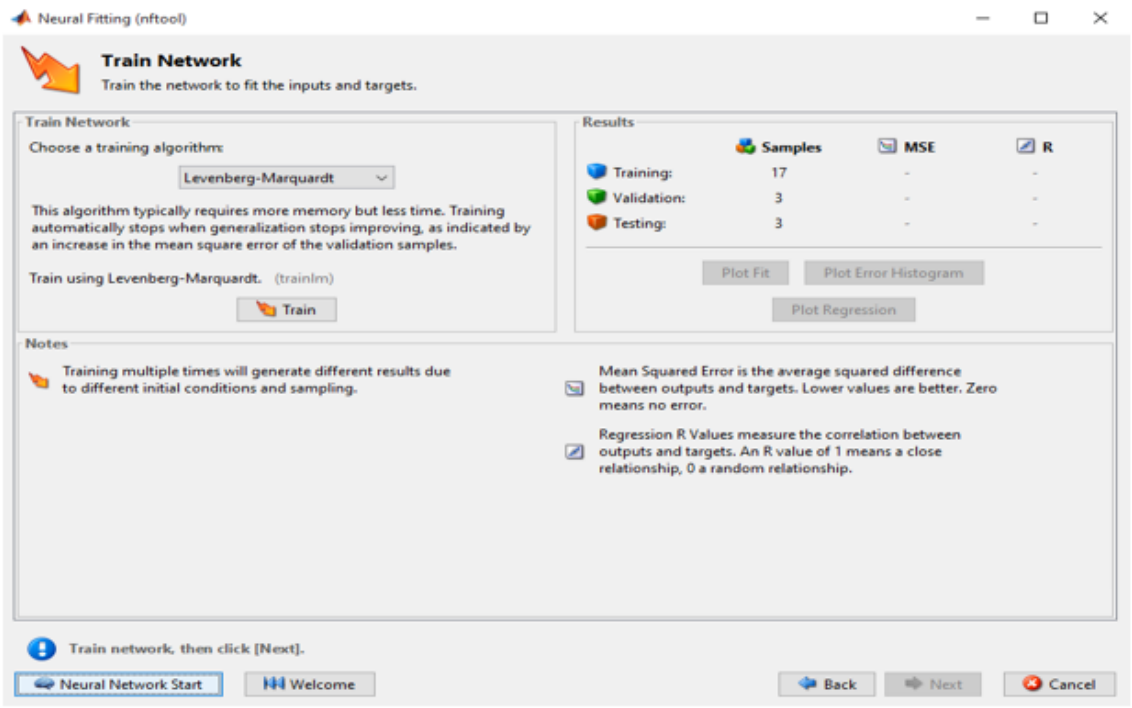

Figure 12. ANN training network interface

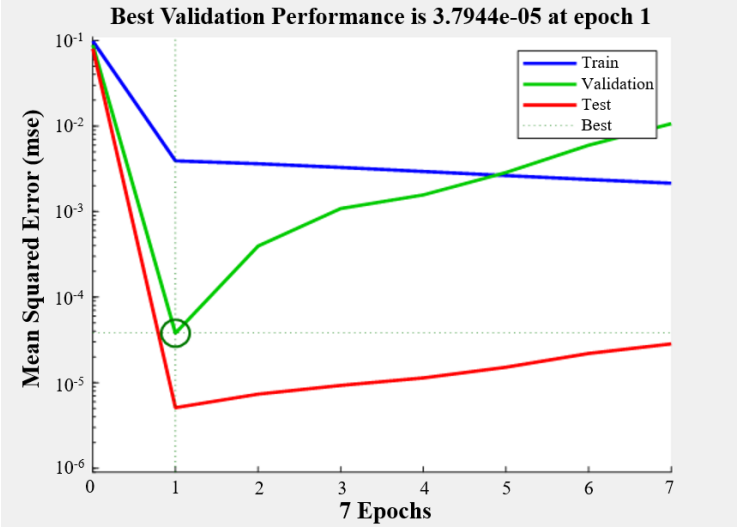

Figure 13. ANN performance plot

Owing to the nature of the dataset, a significantly high enough epoch number could give a better prediction of the dataset, indicating the validity of the adopted ANN training approach. The momentum values (mu) designate the learning rate of the ANN training algorithm. The momentum value, 0.001, indicates quick adoption of the data for training since the learning rate ranges from 0 to 1, and the closer the value to 0, the faster the learning rate.

The NF was utilised because it allows for enhanced modelling, reading, and decision-making within intelligent systems. NF systems function as a powerful tool for addressing complex, uncertain, and dynamic tasks, leveraging the strengths of both neural networks and FL to achieve superior performance. The challenge with NF is that it requires high computational resources.

The error histogram, as depicted in Figure 14, is the deviation of the model prediction from the experimental data. Zero error, as indicated on the plot, indicates the significance and validity of the ANN model to train the acquired dataset. Figure 15 shows the regression plot, which gives the statistical implication of the ANN model. Lastly, the actual data and predicted results for the ANFIS, ANN, and FL models are shown in Figure 16 to demonstrate the superiority of the ANFIS model over other models.

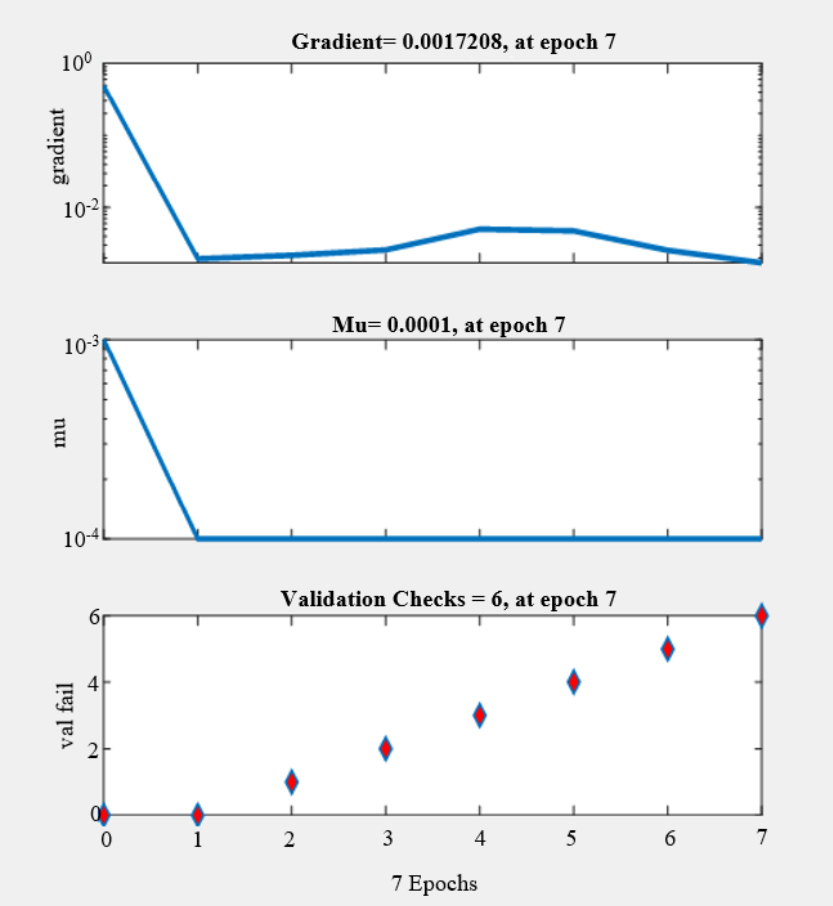

Figure 14. ANN error

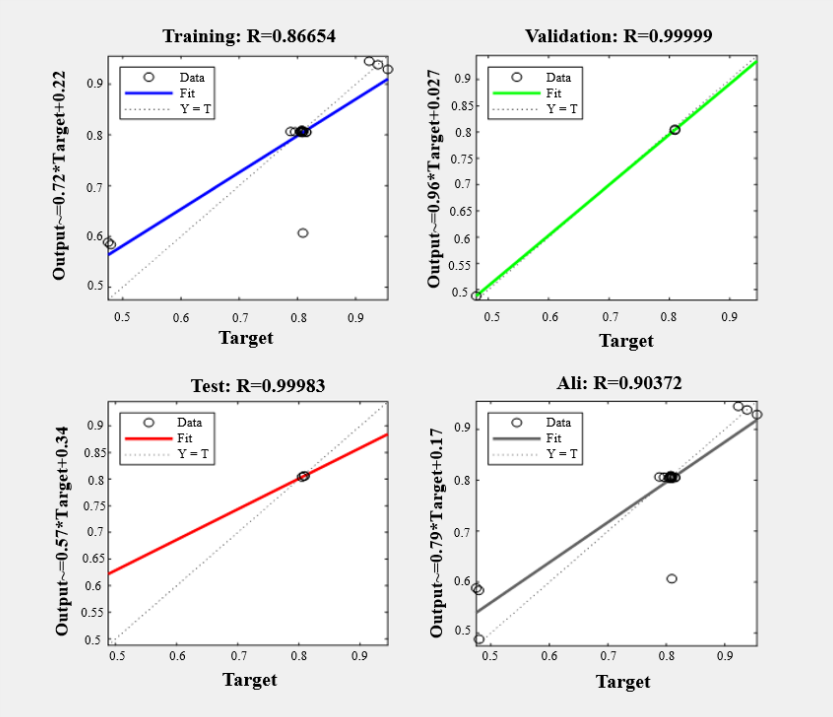

Figure 15. ANN regression

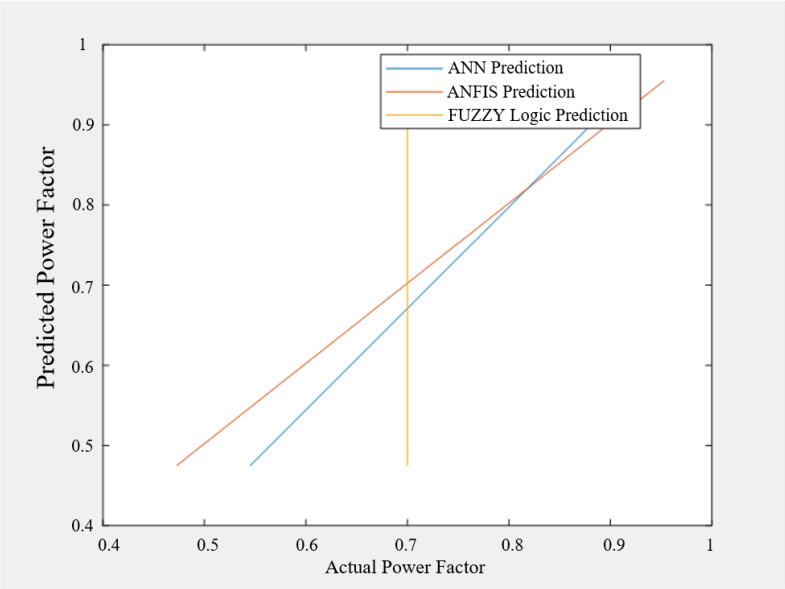

Figure 16. Predicted results of ANFIS, ANN, and FL

However, the NF technique yields superior results compared to other techniques. The challenge of resource-intensive training and fine-turning processes faced with NF requires substantial computational power and memory resources.

5 Conclusions

The neuro-FL controller applied to the switching of the capacitor bank has shown that real-time responses and proactive actions could be taken to further enhance the performance of the PF using the knowledge of artificial intelligence. The forecast was obtained through the experience gained by the controller. On the spot, the effector signal was sent to the actuator for further physical switching. This algorithm, which was trained based on the sub-clustering fuzzy inference system, helped to improve the response speed of the controller at just the 2nd iteration out of 50 epochs. Hence, within the limits of the experimental data and simulation results obtained from this study, it can be concluded that:

i. KVAR and KW are major factors on which the PF depends.

ii. FL strength is fair.

iii. ANNs could perform excellently in terms of the predictive control of the dataset, but ANFIS offers the best training strength, which could be adopted in the prediction, and simultaneous control of the PF of the equipment.

Having considered the results obtained in this study, the following recommendations are made for further research:

i. Disturbance at the point of contact between the actuator and the capacitor bank could be investigated and analyzed.

ii. Implementation of this result could be worked on to save costs further.

Data Availability

The data used to support the research findings are available from the corresponding author upon request.

Conflicts of Interest

The authors declare no conflict of interest.

References

[1] W. Widjonarko, C. Avian, A. Setiawan, M. Rusli, and E. Iskandar, "Capacitor bank controller using artificial neural network with closed-loop system," *Bull. Electr. Eng. Inform.*, vol. 9, no. 4, pp. 1379–1386, 2020. https://doi.org/10.11591/eei.v9i4.2411

[2] A. Miron, A. C. Cziker, and H. G. Beleiu, "Fuzzy control systems for power quality improvement—A systematic review exploring their efficacy and efficiency," *Appl. Sci.*, vol. 14, no. 11, p. 4468, 2024. https://doi.org/10.3390/app14114468

[3] K. M. Rafi, P. V. N. Prasad, and J. V. R. Vithal, "Coordinated control of DSTATCOM with switchable capacitor bank in a secondary radial distribution system for power factor improvement," *J. Electr. Syst. Inf. Technol.*, vol. 9, no. 1, p. 4, 2022. https://doi.org/10.1186/s43067-022-00044-3

[4] M. D. Alsebai and K. K. Pedapenki, "Transformation of type I fuzzy logic into interval type II fuzzy logic-based unit voltage template with controlled load," *Periodica Polytech. Electr. Eng. Comput. Sci.*, vol. 68, no. 1, pp. 37–53, 2024. https://doi.org/10.3311/PPee.22465

[5] Utpal, Rishav, and M. Tiwari, "Automatic power factor correction using capacitor banks," *Int. J. Innov. Res. Electr. Electron. Instrum. Control Eng.*, vol. 4, no. 4, pp. 9–16, 2016. https://doi.org/10.17148/IJIREEICE

[6] A. Sivakumar, M. Thiyagarajan, and K. Kanagarathinam, "Mitigation of supply current harmonics in fuzzy-logic based 3-phase induction motor," *Int. J. Power Electron. Drive Syst.*, vol. 14, no. 1, pp. 266–274, 2023. https://doi.org/10.11591/ijpeds.v14.i1.pp266-274

[7] I. J. Smith and J. Salmon, "High-efficiency operation of an open-ended winding induction motor using constant power factor control," *IEEE Trans. Power Electron.*, vol. 33, no. 12, pp. 10 663–10 672, 2018. https://doi.org/10.1109/TPEL.2018.2806740

[8] S. Padmanaban, S. Chenniappan, and J. B. Holm-Nielsen, *Power Quality in Modern Power Systems*. Academic Press, 2020.

[9] A. Jagan, P. K. Ray, B. P. Behera, and G. Panda, "A fuzzy-logic-based smart power management strategy for reliability enhancement of energy storage system in a hybrid AC-DC microgrid with EV charging station," *Int. J. Emerg. Electr. Power Syst.*, vol. 25, no. 3, pp. 405–419, 2024. https://doi.org/10.1515/ijeeps-2023-0128

[10] S. Saini, P. Sharma, D. K. Dhakad, and L. K. Tripathi, "Power factor correction using bridgeless boost topology," *Int. J. Adv. Eng. Res. Sci.*, vol. 4, no. 4, pp. 209–215, 2017. https://doi.org/10.22161/ijaers.4.4.32

[11] S. K. Kumar Injeti, S. M. Shareef, and T. V. Kumar, "Optimal allocation of DGs and capacitor banks in radial distribution systems," *Distrib. Gen. Altern. Energy J.*, vol. 33, no. 3, pp. 6–34, 2018. https://doi.org/10.1080/21563306.2018.12016723

[12] G. Cabanac, C. Labbé, and A. Magazinov, "Retraction: Inductive load power factor correction using a capacitor bank," *J. Phys.: Conf. Ser.*, vol. 1916, no. 1, p. 012379, 2021. https://doi.org/10.1088/1742-6596/1916/1/012379

[13] O. E. Olabode, I. K. Okakwu, A. S. Alayande, and T. O. Ajewole, "A two-stage approach to shunt capacitor-based optimal reactive power compensation using loss sensitivity factor and cuckoo search algorithm," *Energy Storage*, vol. 2, no. 2, p. e122, 2020. https://doi.org/10.1002/est2.122

[14] C. S. Esobinenwu, "Optimal capacitor placement and sizing for loss minimization in Nigerian power grid using fuzzy logic technique," *Irish J. Eng. A. Sci.*, vol. 7, no. 2, pp. 1–8, 2023.

[15] R. Kumar, P. Sharma, D. Tiwari, and V. Tiwari, "Power factor correction using STATCOM," *Int. J. Recent Eng. Res. Dev. (IJRERD)*, vol. 3, pp. 166–170, 2018.

[16] N. Sharma, M. P. Sharma, S. Singh, and B. Vyas, "Methodology for valuation of shunt capacitor bank in power grid," in *2019 10th International Conference on Computing, Communication and Networking Technologies (ICCCNT)*, Kanpur, India, 2019, pp. 1–7. https://10.1109/ICCCNT45670.2019.8944425

[17] S. Mane, R. Sapat, J. Shelar, R. D. Kulkarni, and J. Mundkar, "Microcontroller based automatic power factor correction system for power quality improvement," in *2020 International Conference for Emerging Technology (INCET)*, Belgaum, India, 2020, pp. 1–6. https://doi.org/10.1109/INCET49848.2020.9154008

[18] K. Kayisli, S. Tuncer, and M. Poyraz, "A novel power factor correction system based on sliding mode fuzzy control," *Electr. Power Compon. Syst.*, vol. 45, no. 4, pp. 430–441, 2017. https://doi.org/10.1080/15325008.2016.1266418

[19] S. Durgadevi and M. G. Umamaheswari, "Adaptive neuro-fuzzy logic controller based current mode control for single phase power factor correction using DC-DC SEPIC converter," in *2017 International Conference on Power and Embedded Drive Control (ICPEDC)*, Chennai, India, 2017, pp. 490–495. https://doi.org/10.1109/ICPEDC.2017.8081139

[20] D. Karaboga and E. Kaya, "Adaptive network based fuzzy inference system (ANFIS) training approaches: A comprehensive survey," *Artif. Intell. Rev.*, vol. 52, no. 4, pp. 2263–2293, 2019. https://doi.org/10.1007/s10462-017-9610-2